Tracing the Heart: An Evidence-Linked Pipeline for Heart-Failure Feature Engineering

Soorya Ram Shimgekar
Nimblemind
Michelle Hu
Nimblemind
Dorisa Shehi
Nimblemind
Daniel Kang
Nimblemind
Roy Ka-Wei Lee
Singapore University of Technology and Design
Koustuv Saha
University of Illinois Urbana-Champaign
Christian Poellabauer
Florida International University
Christopher Lee
University of California Los Angeles
Sajeev Singh
Department of Health Informatics, Rutgers University Newark
Piyum Zonooz
Nimblemind
Navin Kumar
Nimblemind
Zeeshan Ahmed
Rutgers Institute for Health, Health Care Policy and Aging Research
Department of Medicine, Robert Wood Johnson Medical School, Rutgers Health
Priyadarshini Kachroo
Department of Health Informatics, Rutgers University Newark

arXiv:2608.06366v1 [cs.AI] 6 Aug 2026

Abstract

Electronic health record (EHR) feature engineering is a major bottleneck in clinical research and AI, accounting for 39–45% of data scientists' workload. This is especially pronounced in heart failure, which affects an estimated 6.7 million U.S. adults and requires integrating fragmented EHR data with disease-specific, guideline-based clinical reasoning. Existing rule-based and large language model (LLM)-based approaches offer only partial automation with limited maintainability and evidence traceability. We developed the Nimblemind Multi-Agent System (nMAS), an evidence-linked, rubric-grounded pipeline for automated heart-failure feature engineering, and evaluated it on 500 dummy patient records from nine EHR source tables. nMAS generated 132 structured and 70 rubric-scored aggregated features, verified for structural integrity, rubric compliance, and provenance, and audited by a restricted LLM. Adding the aggregated features improved held-out AUROC from 0.895 to 0.963 for HFrEF and 0.870 to 0.910 for HFpEF phenotyping, and an independent LLM-based rubric assessment of evidence support and methodological soundness scored the features at 81.5% of maximum points. These results demonstrate the feasibility of automated, auditable feature engineering for complex cardiovascular EHR data, though evaluation was limited to a single-institution cohort and external validation is needed.

© S.R. Shimgekar *et al.*

Keywords: electronic health records, heart failure, feature engineering, clinical artificial intelligence, multi-agent systems, evidence-linked extraction

1. Introduction

Before a clinical machine-learning model can be trained or a population-level cohort study can be conducted, routinely collected clinical data must be transformed into reliable, analysis-ready patient-level variables. This feature-engineering process involves extracting, cleaning, harmonizing, and deriving variables from heterogeneous clinical records and represents a substantial component of healthcare data-science workflows. Data scientists report spending approximately 39–45% of their working time on data loading and cleaning rather than analysis (Anaconda, 2020). At the median U.S. data-scientist wage of $112,590 per year, or approximately $54 per hour (U.S. Bureau of Labor Statistics, 2026), this corresponds to roughly $845–$975 of labor per 40-hour workweek devoted to data preparation. These costs are further compounded when feature-engineering workflows must be repeatedly reconstructed for new datasets, institutions, or research questions. The resulting lack of reusable data infrastructure remains a barrier to the broader deployment of artificial intelligence (AI) in healthcare (Bian et al., 2026).

Cardiology presents a particularly demanding setting for clinical feature engineering because clinically meaningful variables are distributed across multiple EHR domains and often require longitudinal interpretation. Diagnoses, medications, laboratory measurements, procedures, and imaging findings may be stored in separate relational tables rather than in a single analysis-ready dataset (Kao, 2022). Consequently, constructing patient-level features requires more than extracting individual variables: heterogeneous records must be reconciled, temporally aggregated, and transformed according to clinically meaningful definitions (Roger, 2021). Heart failure (HF) provides a representative case because its characterization depends on multiple complementary sources of clinical evidence and affects a large and growing patient population. An estimated 6.7 million U.S. adults have HF, with prevalence projected to increase to 8.7 million by 2030 (Fonarow et al., 2026). In 2023, HF was mentioned on 452,573 U.S. death certificates, corresponding to 14.6% of all deaths (National Center for Health Statistics, 2025).

HF phenotyping also requires the application of explicit clinical definitions to heterogeneous measurements. Contemporary classifications use guideline-specified thresholds, such as ejection-fraction categories, while other features depend on laboratory measurements, medication histories, comorbidities, and disease-specific scoring criteria (Ostrominski et al., 2024; Maddox et al., 2024). These requirements create a distinction between simply extracting information from an EHR and constructing a clinically meaningful feature: the latter requires explicit rules describing which source variables should be used, how they should be combined, and how the resulting value should be interpreted. For research applications, these transformations must additionally be reproducible and traceable to their underlying source data.

These requirements motivate an automated feature-engineering approach that combines heterogeneous EHR integration with explicit clinical specifications and evidence traceability. We address this need with the Nimblemind Multi-Agent System (nMAS) (Shimgekar et al., 2025b), an evidence-linked, rubric-grounded pipeline for heart-failure feature engineering. Rather than generating unrestricted clinical summaries, nMAS applies deterministic scoring rules derived from clinical specifications and uses a restricted language-model auditing step to evaluate the resulting feature construction. Each derived feature remains linked to its source EHR variables and predefined scoring criteria, enabling automated processing while preserving interpretability and auditability.

In this pilot study, we applied nMAS to 500 dummy heart-failure patient records assembled from nine EHR source tables. We evaluated the resulting dataset for structural integrity, rubric compliance, and clinical coherence. Although downstream predictive performance is reported as a secondary evaluation, the primary objective is to assess whether automated feature engineering produces structurally valid, rubric-compliant, and clinically coherent patient-level features. This study therefore provides preliminary evidence for the feasibility of evidence-linked, rubric-grounded feature generation as a reusable approach for preparing complex cardiovascular EHR datasets.

2. Related Work

Artificial intelligence has been widely applied to diagnosis, risk stratification, and disease management, but most systems operate on a single data modality rather than integrating longitudinal EHR data (Boccuto et al., 2023). Many derive structured clinical variables from a single rich source, such as unstructured clinical documents processed with large language models (Truhn et al., 2024; Balasubramanian et al., 2025), instead of reconciling heterogeneous data across multiple EHR domains. The same pattern exists in cardiology, where AI models have been developed for electrocardiogram-based heart-failure risk prediction (Dhingra et al., 2025). However, these single-modality approaches do not address the preprocessing and integration of structured EHR data required for heart-failure phenotyping, which depends on combining guideline-defined ejection-fraction categories, medication history, laboratory measurements, comorbidities, and other clinical variables across multiple EHR domains (Roger, 2021).

General EHR feature-engineering frameworks address part of this preprocessing challenge but remain disease agnostic. FIDDLE and MIMIC-Extract automate preprocessing and temporal aggregation to generate machine learning-ready representations (Tang et al., 2020; Wang et al., 2020); the OHDSI patient-level prediction framework derives standardized covariates from common clinical domains (Reps et al., 2018); and rule-based methods such as the Charlson and Elixhauser indices engineer comorbidity features from diagnosis codes (Quan et al., 2005). More recent LLM-based approaches relax the rule-based constraint but not the need for guideline-grounded reasoning: FeatEHR-LLM generates feature-extraction code from dataset schemas rather than clinical literature (Karami et al., 2026), while AgentScore learns candidate scoring rules validated statistically against patient data rather than grounded in clinical evidence (Estévez et al., 2026). Consequently, these approaches cannot derive many clinically meaningful heart-failure predictors, including phenotype, disease severity, guideline-directed medical therapy, and care gaps, which require synthesizing diagnoses, medications, laboratory results, imaging, procedures, and behavioral history using guideline-based clinical reasoning.

Few reusable frameworks therefore address the full feature-engineering requirements of cardiovascular research. Heart-failure phenotyping requires integrating diagnoses, medications, laboratory results, imaging, procedures, behavioral history, and guideline-defined ejection-fraction thresholds across longitudinal EHR data. Because these derived variables govern clinical risk stratification, cohort eligibility, and treatment assessment, feature engineering requires both guideline-based clinical reasoning and an auditable link between every derived feature and its supporting evidence.

The present work addresses this gap with an evidence-linked, rubric-grounded pipeline for automated heart-failure feature engineering. Unlike existing frameworks that emphasize generic preprocessing or data-driven rule discovery, our approach encodes guideline-based clinical reasoning within an explicit rubric, integrates heterogeneous EHR evidence into clinically meaningful features, and preserves traceability from each feature to its underlying evidence and source records.

3. Data

The evaluation dataset consisted of 500 dummy patient records drawn from an aggregated cohort modeled on REDACTED, a cardiovascular program serving a minoritized population (Piña et al., 2021). Patients were included if they had a documented heart-failure diagnosis in the source EHR; no additional inclusion or exclusion criteria were applied. Cohort characteristics are summarized in Table 1. Each patient was represented across nine structured EHR tables covering demographics, other diagnoses, medication orders, echocardiogram procedures, surgical procedures, laboratory components and external labs, ejection fraction flowsheet entries, and social history (Table 4 in the Appendix). Direct patient identifiers were replaced with de-identified identifiers before analysis, while clinically relevant information required for feature extraction and phenotyping was preserved.

Each record combined coded administrative and demographic fields (age, sex, race, ethnicity, language, vitals) with free-text clinical fields requiring pattern-based extraction, including ICD-10 code lists, diagnosis names, medication display and pharmacologic-class names, procedure display names, ejection fraction flowsheet text, and social history narrative.

4. Method

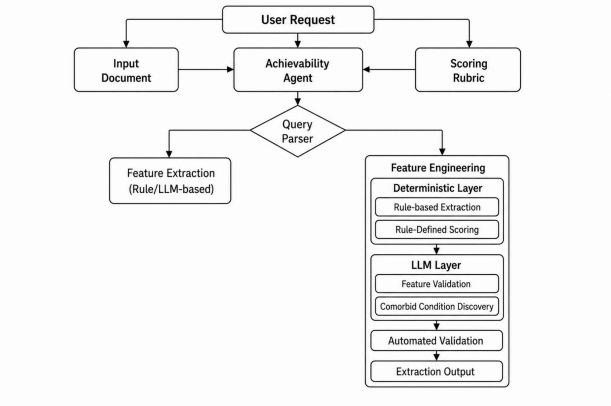

Figure 1: Overview of the nMAS heart-failure feature-extraction pipeline.

Workflow Overview. As shown in Figure 1, the workflow begins with a request specifying the input EHR exports and constructs the target features defined in the versioned rubric. The Achievability Agent first checks that the available source data can support each target feature; features whose required inputs are absent are reported as unsupported rather than assigned inferred values. For supported requests, the Query Parser then routes the request to one of several nMAS pipelines (Shimgekar et al., 2025b); for brevity, we provide two representative pipelines here: feature extraction and feature engineering.

In the feature-extraction pipeline, each field is routed through rule/LLM-based extraction tiers, depending on how much contextual interpretation the field requires, and returns the field's value directly from the source document along with a verbatim source sentence confirming that value (Wang et al., 2026). Feature engineering instead composes extracted values into rubric-scored, evidence-linked composite variables that remain traceable to their source data and to the guideline literature that justifies them. This paper focuses exclusively on the feature-engineering pipeline, in which supported features are produced in two stages, with routing driven by the configured rubric and field definitions rather than by any downstream label. Stage 1 builds a single patient-level table from the EHR source tables: (1) standardizes each table (whitespace, null tokens, uppercased identifiers, and ISO datetimes); (2) deduplicates each table on a clinically meaningful event key; (3) temporally aggregates each source to the patient level independently; (4) Merges per-table summaries into unique patient rows.

Stage 2 enriches this table with higher-order composite features: (1) produces the higher-order feature categories described below, including a comorbidburden category spanning five organ systems, each returned as a compact value paired with a structured evidence trace; (2) reviews composite features with an LLM auditor; (3) checks structural integrity, rubric compliance, monotonicity, and evidence traceability before release.

Input Standardization and Deduplication. Before aggregation, every source table was converted into a consistent representation. String columns were whitespace-collapsed and trimmed, empty strings and literal `"nan"` tokens were converted to null, and patient identifiers were uppercased so that keys join reliably. EHR-style datetime fields (for example, `03-Apr-24 06.00.00.000000 AM`) were parsed into a unified ISO representation (`2024-04-03 06:00:00`), which is required for correct temporal ordering, first/latest event extraction, and recurrence analysis.

Each table was deduplicated using clinically meaningful event keys to prevent repeated exports or reorders from inflating counts. The source tables and keys are listed in Appendix Table 5. Deduplication preceded aggregation so that, for example, resent medications and retransmitted laboratory results were not double counted.

Patient-Level Temporal Aggregation. Each source was collapsed to the patient level first, computing counts, first and latest event timestamps, and clinically relevant flags. Table 6 in the Appendix lists the quantities produced from each event source.

Ejection fraction is often recorded as a range (Ostrominski et al., 2024), so each entry was parsed into a low bound, a high bound, and a midpoint ("20–25%" becomes 20, 25, and 22.5), from which the lowest, highest, and most-recent EF were computed, plus a flag for latest recordings with conflicting values. On merging, every continuous measurement (EF, BNP, troponin, BMI, blood pressure) received an availability indicator, and missing values were kept missing rather than set to zero, since a zero EF would read as profound systolic dysfunction and inflate the severity scores. The merge was validated to keep one row per patient and preserve the input row count.

Clinical Feature Engineering. Before scoring, a clinical-reasoning layer converted raw text and codes into interpretable flags (Table 7 in the Appendix). Two choices are worth noting. First, behavioral exposures were kept as ordered categories rather than binary flags, because cardiovascular risk from tobacco and alcohol persists after cessation and varies by intensity (Yoo et al., 2023; Piano et al., 2025). Second, the heart-failure phenotype was dictated by ICD-derived values rather than diagnosis names, carrying a conflict flag when the two disagreed (Quan et al., 2005).

Composite Feature Generation. In Stage 2, the pipeline generates composite features by applying a versioned clinical scoring rubric to Stage 1 variables. These features summarize multiple clinical inputs into interpretable scores, counts, and indices while preserving their contributing evidence. The rubric defines the conditions, point assignments, and evidence hierarchy used to transform structured EHR data into interpretable feature scores.

Table 3 in the Appendix provides the complete point structure for all eight feature categories, including each component's condition and point value. A representative portion of the underlying JSON representation is shown in Figure 2 in the Appendix.

The rubric was developed using `Qwen 2.5-1.5B-Instruct`, which assembled recent guideline-level literature into a proposed scoring framework. A professional cardiologist then reviewed and approved the rubric in full. The final version included 22 references from 2023 onward, sourced from leading cardiovascular and specialty journals, with each reference linked to the component it supports.

The scoring system preserves clinically meaningful ordering across structured variables. The weights distinguish: (1) direct evidence from supportive evidence; (2) current findings from historical information; (3) independent features from overlapping measurements; and (4) feature-specific variables from cross-system modifiers. The assigned point values represent an interpretable engineering design informed by clinical literature rather than quantities directly derived from published studies.

In general, direct diagnostic evidence receives the highest weight within each category. Supportive laboratory findings and cross-system modifiers contribute smaller, capped amounts. For example, hypertension diagnosis contributes fewer cardiovascular risk points because measured blood pressure is scored separately. Elevated natriuretic peptide and troponin increase disease severity because they reflect worsening cardiac structure and function (Myhre et al., 2024). Current tobacco use receives greater weight than former use because smoking cessation reduces heart failure risk (Yoo et al., 2023). Alcohol use is ordered by consumption intensity following American Heart Association guidance (Piano et al., 2025). Age and blood pressure weights follow contemporary cardiovascular risk equations validated across diverse populations (Lewis et al., 2025). Demographic vulnerability variables are included only as administrative equity review factors rather than biological risk measures (Bazoukis et al., 2025).

After validation, patient data are processed through the deterministic scoring engine using the finalized rubric. Seven of the eight category features use the same scoring approach. These include disease severity, cardiovascular risk, the five comorbidburden scores (kidney, lungs, metabolic, blood, and brain-health context), and demographic vulnerability. Each feature sums component points, caps the total at 100, and maps the score to an ordinal label. Scores of 55 or above are classified as high, 25 to 54 as medium, and below 25 as low. Each feature also returns the contributing components, assigned points, plain-language explanations, source columns, and whether required inputs were present. This ensures that every aggregated value remains auditable.

The heart-failure phenotype feature uses a separate logic because ejection-fraction classes are categorical thresholds rather than weighted composites. The phenotype is assigned using a precedence rule over available evidence. When numeric EF is present, it directly determines the phenotype: heart failure with reduced ejection fraction (HFrEF) at midpoint ≤ 40, heart failure with mildly reduced ejection fraction (HFmrEF) below 50, and heart failure with preserved ejection fraction (HFpEF) otherwise, following contemporary guideline EF categories (Ostrominski et al., 2024). When EF is unavailable, the pipeline uses ICD-10 diagnosis codes for systolic, diastolic, or combined heart failure without imputing an EF value. A patient is never assigned both reduced and preserved phenotypes. This same numeric-or-diagnosis-only logic determines eligibility for HFrEF-specific care-gap checks, keeping guideline-directed therapy recommendations aligned with available evidence (Maddox et al., 2024).

LLM Rubric-Auditor Validation and Correction. Because composite features encode clinical

reasoning that deterministic rules may approximate imperfectly, each candidate row is audited by `Qwen 2.5-1.5B-Instruct`. The prompt provides patient evidence, the candidate row, and a whitelist of correctable fields; the model returns `{"valid": true}` when the row is correct or a minimal `corrections` object otherwise. Only whitelisted numeric and categorical fields may be modified (Table 9 in the Appendix); fields ending in `_json` or `_explanation` are protected to preserve deterministic evidence traces and rationales. Corrections are type-coerced before application, while unparseable responses are logged as audit failures and leave the original scores unchanged. The prompt template is provided in Figure 3 in the Appendix.

The auditor runs locally, and each row records the model, raw response, and `generated_*` status, ensuring that auditing is a required and traceable pipeline step rather than an optional post-processing stage.

Comorbid Condition Discovery. A final stage catalogs conditions beyond heart failure that the dataset can model. Candidate conditions are fixed in the rubric (13 cardiovascular and comorbid conditions, each tagged by clinical group and evidence type), so the stage selects supporting evidence rather than discovering new conditions. For each candidate, the pipeline considers only merged and higher-order columns in the final dataset, excludes conditions without supporting columns, and prompts the language model, under the auditor's guardrails, to identify evidence-bearing columns and explain their relevance. The model cannot add conditions, invent columns, or label patients; returned columns are validated against the dataset, with a deterministic fallback for unusable responses. The resulting condition-prediction catalog and prompt template are provided in Figure 4 in the Appendix.

Quality Assurance and Evaluation. The enriched dataset was validated using an automated evaluation harness that performs structural, clinical, and provenance checks and generates a machine-readable report of identified issues. The harness verifies: (1) unique patient identifiers and valid table joins; (2) valid and mutually exclusive heart-failure phenotype indicators; (3) preservation of missing values; (4) compliance with the scoring rubric by independently checking selected scores against predefined thresholds and formulas defined in Figure 2; (5) expected scoring behavior, such as higher scores for current versus former tobacco use; (6) complete traceability of score components; and (7) provenance of generated features and supporting references.

Multi-Agent System Evaluation. To evaluate whether aggregated features improve prediction beyond cleaned EHR variables alone, we trained XGBoost classifiers (Chen and Guestrin, 2016) for two binary tasks: HFrEF (reduced ejection fraction, EF ≤ 40) versus phenotype-unknown and HFpEF (preserved ejection fraction, EF ≥ 50) versus phenotype-unknown. As described in Section 3, this cardiovascular program serves a minoritized population where limited access to diagnostic imaging and specialist follow-up can leave heart failure documented without definitive phenotype assignment (Piña et al., 2021). Consequently, a representative non-heart-failure control cohort was unavailable for this pilot study. Phenotype-unknown patients had documented heart failure but insufficient evidence to assign HFrEF, HFmrEF, or HFpEF; thus, the evaluation assessed heart-failure phenotyping rather than disease diagnosis.

For each task, we compared a baseline containing only cleaned and merged structured variables with an aggregated feature set that additionally included the composite features. XGBoost was chosen because it natively handles missing values during split selection, eliminating explicit imputation. All models used identical hyperparameters (Appendix A.3).

Models were evaluated using 5-fold stratified cross-validation repeated 10 times with independent shuffles (50 test evaluations per model). The same fold assignments were reused for both feature sets within each task to enable paired comparisons on identical patients. We report mean $\pm$ standard deviation for accuracy, AUROC, and F1 score across test folds. Feature contributions were quantified using global TreeSHAP values (Lundberg and Lee, 2017).

LLM-Based Evaluation. To assess feature quality beyond predictive performance, we performed a structured construct-validity evaluation of every engineered rubric component using Claude Opus 4.8 and a five-dimensional rubric. The evaluation assessed external evidence support, methodological soundness, reproducibility, and EHR data reliability, complementing downstream classification results. The complete rubric, procedure, system prompt, metadata, and results are provided in Appendix A.6.

Comparator and ablation studies. We conducted two additional analyses: an ablation study measuring the contribution of individual feature categories and rubric design choices, and an indepen-

dent comparator where an LLM engineered features directly from raw EHR data. Full methodologies, results, and prompts are provided in Appendix A.10 and Appendix A.9.

5. Results

Structured Merge. Stage 1 collapsed nine source tables to the patient level without Cartesian explosion, producing exactly one row per patient, no duplicates, and 132 structured columns across all 500 patients. The engineered features showed coherent cohort-level distributions (Table 1): cardiovascular comorbidities were common, while key measurements remained sparse. Notably, numeric ejection fraction was available for only 3.0% of patients, requiring diagnosis-name fallback for phenotype assignment.

Table 1: Characteristics of the 500-patient development cohort. Values shown are dummy data for illustration.

Characteristic	Value
Total patients	500
Sex	
Male	256 (51.2%)
Female	243 (48.6%)
Unspecified	1 (0.2%)
Mean BMI (n=266)	29.99
Documented comorbidities	
Chronic kidney disease	227 (45.4%)
Diabetes	208 (41.6%)
Coronary artery disease	202 (40.4%)
Atrial fibrillation	175 (35.0%)
Measurement availability	
Numeric ejection fraction	15 (3.0%)
BNP / NT-proBNP	154 (30.8%)
Troponin	429 (85.8%)

Higher-Order Composite Features. Stage 2 generated the feature categories in Table 3 as 70 columns, with all 500 rows audited by `Qwen 2.5-1.5B-Instruct`. Each feature included a structured evidence trace documenting contributing components, point values, source columns, and input availability. The categories produced two output types, illustrated by representative examples.

The first was a scored assessment with ranked drivers, shown in Figure 6 using the disease-severity feature. Because this patient lacked numeric ejection fraction, phenotype was inferred from diagnosis text (`HFpEF_by_diagnosis_name`, source `DXNAMES`). The resulting score was driven by elevated natriuretic peptide levels, abnormal troponin results, and chronic kidney disease, each recorded as a source-linked contributor.

The second output type was a documentation-gap list, shown in Figure 7. The care-recommendation feature identifies evidence columns associated with each gap and frames outputs as documentation review rather than prescriptive advice. For example, a patient with coronary artery disease but no statin flag received a high-urgency statin documentation review prompt, along with prompts to review potassium, creatinine, and sodium monitoring.

Comorbid Condition Discovery. The condition-discovery stage indicates which other conditions the enriched dataset could support for modeling. It produced a catalog of thirteen candidate conditions spanning cardiac, vascular, metabolic, renal, pulmonary, and hematologic domains, for example hypertension, diabetes, chronic kidney disease, coronary artery disease, atrial fibrillation, anemia, and COPD. For each, it listed the merged and higher-order columns present in the final dataset that could serve as modeling evidence, together with a generated rationale and no patient-level diagnoses. The anemia entry in the Appendix (Figure 5) is representative: an anemia diagnosis flag, hemoglobin laboratory summaries, and blood and kidney comorbid-burden features together support modeling that condition.

Evaluation Performance. Table 2 summarizes the 5-fold cross-validated performance of the baseline and aggregated feature sets. Adding the composite features improved performance for both classification tasks across all evaluation metrics. The largest improvement was observed for HFrEF classification, with accuracy increasing from 0.776 to 0.896 (+0.120). HFpEF classification also improved across all evaluated metrics, although the gains were smaller, with accuracy increasing from 0.752 to 0.809 (+0.057).

Global feature importance was assessed using mean absolute SHAP values. For HFrEF classification, 6 of the top 10 features were composite features generated by the proposed framework, with demographic vulnerability adjusted gap and disease severity adjusted gap ranking above the highest-ranked baseline feature, HF GDMT medication class count. For HFpEF,

Table 2: Held-out cross-validated performance (mean ± std across 5 folds, repeated 10 times) for baseline versus aggregated feature sets, for each phenotype classification task.

Task	Features	Accuracy	AUROC	F1
HFrEF	Baseline	0.776 ± 0.065	0.895 ± 0.046	0.776 ± 0.063
	Aggregated	0.896 ± 0.049	0.963 ± 0.028	0.894 ± 0.052
HFpEF	Baseline	0.752 ± 0.056	0.870 ± 0.042	0.758 ± 0.058
	Aggregated	0.809 ± 0.061	0.910 ± 0.040	0.812 ± 0.059

two composite features appeared in the top 10, with disease severity score as the most influential composite predictor and troponin abnormal count remaining the dominant baseline feature. Complete SHAP rankings are provided in Table 12 in the Appendix.

The LLM-based construct-validity assessment showed strong overall performance, with most categories exceeding 85% and an overall normalized score of 81.5% (Table 11). Lower scores were observed for demographic vulnerability and gap features, with care recommendations receiving the lowest score (38.5

To determine whether performance gains reflected clinically grounded feature weighting rather than feature count alone, equal-weight and random-weight ablations fixed the aggregated feature set while varying only the scoring logic. Both substantially reduced performance (Appendix A.10), indicating that rubric weighting contributed to the improvement. Full ablation and comparator analyses are reported in Appendix A.10 and Appendix A.9.

6. Discussion

We developed a pipeline that transforms fragmented EHR exports into a patient-level heart-failure cohort with rubric-derived, evidence-linked feature categories. Adding these features improved HFrEF accuracy, AUROC, and F1 score by 0.120, 0.068, and 0.118, respectively, and HFpEF performance by 0.057, 0.040, and 0.054, respectively. Independent literature-grounded grading scored seven of eleven feature categories above 85/100. Feature-importance analysis showed that rubric-derived features accounted for 6 of the top 10 HFrEF predictors and 2 of the top 10 HFpEF predictors, suggesting they captured information beyond the original structured variables.

Although not designed for clinical decision support, the generated features may support identification of patients relevant to established care pathways. For example, care-gap checks identify reduced-EF heart-failure patients lacking guideline-directed medical therapy, a population relevant to optimization strategies such as STRONG-HF (Mebazaa et al., 2022), while kidney comorbidity features may help identify patients who could benefit from earlier nephrology referral, which has been associated with improved outcomes in observational studies and meta-analyses (Cheng et al., 2025). These represent potential applications rather than measured clinical effects.

Beyond predictive performance, the pipeline provides a reproducible and auditable approach for clinical data preparation. The generated features retain links to their source variables, scoring criteria, and supporting evidence, enabling transparent review of how each feature was constructed. This design separates clinical knowledge representation from feature execution, allowing the scoring framework to be updated independently from the underlying data-processing pipeline. The same separation makes the approach reusable well beyond heart failure. Any data-intensive chronic disease facing the same feature-engineering bottleneck could substitute its own guideline-grounded rubric into this scoring engine without rebuilding the extraction and auditing infrastructure underneath it. The condition-discovery catalog is one concrete instance of this reusability, extending the framework across thirteen cardiovascular conditions and allowing future studies to reuse feature-generation methods rather than repeat manual preparation.

Constructing analysis-ready cohorts from fragmented EHR exports remains a major bottleneck in clinical research. As noted in Section 1, data preparation accounts for a substantial portion of data scientists' time (Anaconda, 2020), making reusable,

version-controlled pipelines valuable for reducing repetitive manual work. This burden extends to clinical workflows: in a heart-failure clinical trial prescreening effort, manual eligibility review took approximately 15–20 minutes per patient, with screening of 198 patients requiring two weeks of coordinator effort (Adupa et al., 2016).

The pipeline combines deterministic, guideline-grounded scoring with bounded model-assisted rubric generation and auditing. Rule-based approaches provide transparency but can become brittle as schemas evolve (Wang et al., 2018), whereas large language models offer flexible clinical abstraction but may produce unsupported outputs (Ji et al., 2023). By combining structured execution with evidence-linked rubric development, this framework extends prior evidence-linked clinical AI approaches (Shimgekar et al., 2025b,a; Vassef et al., 2025; Wang et al., 2026) toward reusable EHR feature engineering.

Several limitations should be considered. The pipeline was evaluated on a dummy, single-institution cohort of 500 patients, limiting statistical power and external generalizability. HFrEF and HFpEF were classified against phenotype-unknown patients rather than non-HF controls, so performance reflects phenotype characterization within an HF cohort rather than general disease detection. Evaluation focused on internal consistency, feature traceability, and downstream classification rather than external clinical validity, and some aggregated features incorporate phenotype-related evidence, creating potential feature-label overlap in performance and ablation analyses. Prospective clinical impact and patient outcomes were not assessed. Comorbidity and behavioral features rely partly on regular-expression matching and may miss atypical or institution-specific language. Finally, clinician review covered the extraction rubric and representative outputs rather than the full cohort.

Future work should evaluate the pipeline on larger, multi-institutional cohorts with temporally separated validation sets to assess generalizability. Broader evaluation should include both heart-failure and non-heart-failure populations, independent clinician-adjudicated phenotypes, and additional phenotyping and outcome-prediction tasks, as well as prospective workflow impact (Collins et al., 2024). Until such validation, the pipeline should remain an evidence-linked feature-engineering layer for research and clinical review rather than autonomous clinical decision-making.

References

Abhishek Kalyan Adupa, Ravi Prakash Garg, Jessica Corona-Cox, Sanjiv. J. Shah, and Siddhartha R. Jonnalagadda. An information extraction approach to prescreen heart failure patients for clinical trials, 2016. URL https://arxiv.org/abs/1609.01594.

Anaconda. 2020 state of data science: Moving from hype toward maturity, 2020. URL https://www.anaconda.com/resources/whitepaper/state-of-data-science-2020. Accessed: July 9, 2026. Reported that data scientists spend an average of 45% of their time loading and cleansing data.

J. B. Balasubramanian, D. Adams, I. Roxanis, Ana B. de Gonzalez, P. Coulson, J. S. Almeida, and M. García-Closas. Leveraging large language models for structured information extraction from pathology reports. *Journal of Pathology Informatics*, 19:100521, 2025. doi: 10.1016/j.jpi.2025.100521. URL https://doi.org/10.1016/j.jpi.2025.100521.

G. Bazoukis, J. Loscalzo, J. L. Hall, S. C. Bollepalli, J. P. Singh, and A. A. Armoundas. Impact of social determinants of health on cardiovascular disease. *Journal of the American Heart Association*, 14(5): e039031, 2025. doi: 10.1161/JAHA.124.039031.

Jiang Bian, Majid Afshar, Catherine M. Scifres, et al. The bottleneck was never data or algorithms: Building a learning utility for ai-enabled learning health systems. *npj Health Systems*, 3: 43, 2026. doi: 10.1038/s44401-026-00107-x. URL https://doi.org/10.1038/s44401-026-00107-x.

Francesco Boccuto, Salvatore De Rosa, Danilo Torella, Pierangelo Veltri, and Pietro H. Guzzi. Will artificial intelligence provide answers to current gaps and needs in chronic heart failure? *Applied Sciences*, 13(13):7663, 2023. doi: 10.3390/app13137663. URL https://doi.org/10.3390/app13137663.

Tianqi Chen and Carlos Guestrin. Xgboost: A scalable tree boosting system. In *Proceedings of the 22nd ACM SIGKDD International Conference on Knowledge Discovery and Data Mining*, KDD '16, page 785–794. ACM, August 2016. doi: 10.1145/2939672.2939785. URL http://dx.doi.org/10.1145/2939672.2939785.

L. Cheng, N. Hu, D. Song, L. Liu, and Y. Chen. Early versus late nephrology referral and patient outcomes in chronic kidney disease: An updated systematic review and meta-analysis. *BMC Nephrology*, 26(1):25, 2025. doi: 10.1186/s12882-025-03944-4. URL https://doi.org/10.1186/s12882-025-03944-4.

Gary S. Collins, Karel G. M. Moons, Paula Dhiman, Richard D. Riley, Andrew L. Beam, Ben Van Calster, Marzyeh Ghassemi, Xiaoxuan Liu, Johannes B. Reitsma, Maarten van Smeden, Anne-Laure Boulesteix, Jennifer C. Camaradou, Leo Anthony Celi, Spiros Denaxas, Alastair K. Denniston, Ben Glocker, Robert M. Golub, Hugh Harvey, Georg Heinze, Michael M. Hoffman, Andre Pascal Kengne, Emily Lam, Naomi Lee, Elizabeth W. Loder, Lena Maier-Hein, Bilal A. Mateen, Melissa D. McCradden, Lauren Oakden-Rayner, Johan Ordish, Richard Parnell, Sherri Rose, Karandeep Singh, Laure Wynants, and Patricia Logullo. Tripod+ai statement: updated guidance for reporting clinical prediction models that use regression or machine learning methods. *BMJ*, 385:q902, 2024. doi: 10.1136/bmj.q902.

Lovedeep S. Dhingra, Arya Aminorroaya, Veer Sangha, Aline F. Pedroso, Folkert W. Asselbergs, Luisa C. C. Brant, Sandhi M. Barreto, Antonio Luiz P. Ribeiro, Harlan M. Krumholz, Evangelos K. Oikonomou, and Rohan Khera. Heart failure risk stratification using artificial intelligence applied to electrocardiogram images: A multinational study. *European Heart Journal*, 46(11):1044–1053, 2025. doi: 10.1093/eurheartj/ehae914. URL https://doi.org/10.1093/eurheartj/ehae914.

Silas Ruhrberg Estévez, Christopher Chiu, and Mihaela van der Schaar. Automatic construction of clinical scoring systems with llm agents, 2026. URL https://arxiv.org/abs/2601.22324.

Gregg C. Fonarow, Faraz S. Ahmad, Tariq Ahmad, et al. HF STATS 2025: Heart Failure Epidemiology and Outcomes Statistics: An Updated 2025 Report from the Heart Failure Society of America. *Journal of Cardiac Failure*, 32(2):439–498, February 2026. doi: 10.1016/j.cardfail.2025.07.007. URL https://doi.org/10.1016/j.cardfail.2025.07.007.

Ziwei Ji, Nayeon Lee, Rita Frieske, Tiezheng Yu, Dan Su, Yan Xu, Etsuko Ishii, Ye Jin Bang, Andrea Madotto, and Pascale Fung. Survey of hallucination in natural language generation. *ACM Computing Surveys*, 55(12):1–38, March 2023. ISSN 1557-7341. doi: 10.1145/3571730. URL http://dx.doi.org/10.1145/3571730.

M. G. Kahn, T. J. Callahan, J. Barnard, A. E. Bauck, J. Brown, B. N. Davidson, H. Estiri, C. Goerg, E. Holve, S. G. Johnson, S. T. Liaw, M. Hamilton-Lopez, D. Meeker, T. C. Ong, P. Ryan, N. Shang, N. G. Weiskopf, C. Weng, M. N. Zozus, and L. Schilling. A harmonized data quality assessment terminology and framework for the secondary use of electronic health record data. *EGEMS (Washington, DC)*, 4(1):1244, 2016. doi: 10.13063/2327-9214.1244.

David P. Kao. Electronic health records and heart failure. *Heart Failure Clinics*, 18(2):201–211, April 2022. doi: 10.1016/j.hfc.2021.12.004. URL https://doi.org/10.1016/j.hfc.2021.12.004.

Hojjat Karami, David Atienza, Jean-Philippe Thiran, and Anisoara Ionescu. Featehr-llm: Leveraging large language models for feature engineering in electronic health records, 2026. URL https://arxiv.org/abs/2604.22534.

A. A. Lewis, A. M. Bacong, L. Palaniappan, and T. Hernandez-Boussard. Validation of the american heart association predicting risk of cardiovascular disease events equations in diverse socioeconomic groups: The all of us cohort. *Journal of the American Heart Association*, 14(18):e041549, 2025. doi: 10.1161/JAHA.125.041549.

Scott Lundberg and Su-In Lee. A unified approach to interpreting model predictions, 2017. URL https://arxiv.org/abs/1705.07874.

Thomas M. Maddox, James L. Jr. Januzzi, Larry A. Allen, Khadijah Breathett, Sarah Brouse, Javed Butler, Lori L. Davis, Gregg C. Fonarow, Nasrien E. Ibrahim, JoAnn Lindenfeld, Frederick A. Masoudi, Shubha R. Motiwala, Edwin Oliveros, Michael N. Walsh, Andrew Wasserman, Clyde W. Yancy, and Quinn R. Youmans. 2024 acc expert consensus decision pathway for treatment of heart failure with reduced ejection fraction: A report of the american college of cardiology solution set oversight committee. *Journal of the American College of Cardiology*, 83(15):1444–1488, 2024. doi: 10.1016/j.jacc.2023.12.024.

T. G. McGinn, G. H. Guyatt, P. C. Wyer, C. D. Naylor, I. G. Stiell, and W. S. Richardson. Users' guides to the medical literature: Xxii: How to use articles about clinical decision rules. *JAMA*, 284 (1):79–84, 2000. doi: 10.1001/jama.284.1.79.

A. Mebazaa, B. Davison, O. Chioncel, A. Cohen-Solal, R. Diaz, G. Filippatos, M. Metra, P. Ponikowski, K. Sliwa, A. A. Voors, C. Edwards, M. Novosadova, K. Takagi, A. Damasceno, H. Saidu, E. Gayat, P. S. Pang, J. Celutkiene, and G. Cotter. Safety, tolerability and efficacy of up-titration of guideline-directed medical therapies for acute heart failure (strong-hf): A multinational, open-label, randomised, trial. *The Lancet*, 400(10367):1938–1952, 2022. doi: 10.1016/S0140-6736(22)02076-1.

P. L. Myhre, B. Claggett, C. M. Ballantyne, R. C. Hoogeveen, E. Selvin, K. Matsushita, D. Kitzman, S. Konety, T. Mosley, and A. M. Shah. Nt-probnp and cardiac troponin i, but not cardiac troponin t, are associated with 7-year changes in cardiac structure and function in older adults: The aric study. *Circulation*, 150(23):1847–1857, 2024. doi: 10.1161/CIRCULATIONAHA.124.069735.

Claude Nadeau and Yoshua Bengio. Inference for the generalization error. *Machine Learning*, 52(3):239–281, 2003. doi: 10.1023/A:1024068626366.

National Center for Health Statistics. Multiple cause of death 2018–2023 on cdc wonder database, 2025. URL https://wonder.cdc.gov/mcd.html. Accessed: February 1, 2025. In 2023, heart failure was mentioned on 452,573 death certificates, accounting for 14.6% of all U.S. deaths.

John W. Ostrominski, Ersilia M. DeFilippis, Kannu Bansal, Ralph J. III Riello, Biykem Bozkurt, Paul A. Heidenreich, and Muthiah Vaduganathan. Contemporary american and european guidelines for heart failure management: JACC: Heart failure guideline comparison. *JACC: Heart Failure*, 12(5):810–825, May 2024. doi: 10.1016/j.jchf.2024.02.020. URL https://doi.org/10.1016/j.jchf.2024.02.020.

M. R. Piano, G. M. Marcus, D. M. Aycock, J. Buckman, C. L. Hwang, S. C. Larsson, K. J. Mukamal, and M. Roerecke. Alcohol use and cardiovascular disease: A scientific statement from the american heart association. *Circulation*, 152(1):e7–e21, 2025. doi: 10.1161/CIR.0000000000001341.

I. L. Piña, S. Jimenez, E. F. Lewis, A. A. Morris, A. Onwuanyi, E. Tam, and H. O. Ventura. Race and ethnicity in heart failure: Jacc focus seminar 8/9. *Journal of the American College of Cardiology*, 78(25):2589–2598, 2021. doi: 10.1016/j.jacc.2021.06.058.

Hude Quan, Vijaya Sundararajan, Patricia Halfon, Andrew Fong, Bernard Burnand, Jean-Christophe Luthi, Lesley D. Saunders, Cynthia A. Beck, Thomas E. Feasby, and William A. Ghali. Coding algorithms for defining comorbidities in icd-9-cm and icd-10 administrative data. *Medical Care*, 43(11):1130–1139, 2005. doi: 10.1097/01.mlr.0000182534.19832.83. URL https://doi.org/10.1097/01.mlr.0000182534.19832.83.

Jennifer M. Reps, Martijn J. Schuemie, Marc A. Suchard, Patrick B. Ryan, and Peter R. Rijnbeek. Design and implementation of a standardized framework to generate and evaluate patient-level prediction models using observational healthcare data. *Journal of the American Medical Informatics Association*, 25(8):969–975, 2018. doi: 10.1093/jamia/ocy032. URL https://doi.org/10.1093/jamia/ocy032.

Véronique L. Roger. Epidemiology of heart failure: A contemporary perspective. *Circulation Research*, 128(10):1421–1434, 2021. doi: 10.1161/CIRCRESAHA.121.318172. URL https://doi.org/10.1161/CIRCRESAHA.121.318172.

Soorya Ram Shimgekar, Abhay Goyal, Shayan Vassef, Koustuv Saha, Christian Poellabauer, Xavier Vautier, Pi Zonooz, and Navin Kumar. Nimblelabs: Accelerating healthcare ai development through agentic ai. In *2025 IEEE International Conference on Big Data (BigData)*, pages 8327–8329, 2025a. doi: 10.1109/BigData66926.2025.11401464.

Soorya Ram Shimgekar, Shayan Vassef, Abhay Goyal, Navin Kumar, and Koustuv Saha. Agentic ai framework for end-to-end medical data inference, 2025b. URL https://arxiv.org/abs/2507.18115.

Shengpu Tang, Pedram Davarmanesh, Yang Song, Danai Koutra, Michael W. Sjoding, and Jenna Wiens. Democratizing ehr analyses with fiddle: A flexible data-driven preprocessing pipeline for structured clinical data. *Journal of the American Medical Informatics Association*, 27(12):1921–

1934, 2020. doi: 10.1093/jamia/ocaa139. URL https://doi.org/10.1093/jamia/ocaa139.

Daniel Truhn, Christian M. Loeffler, Gustav Müller-Franzes, Sven Nebelung, Kevin J. Hewitt, Sebastian Brandner, Keno K. Bressem, Sebastian Foersch, and Jakob N. Kather. Extracting structured information from unstructured histopathology reports using generative pre-trained transformer 4 (GPT-4). *The Journal of Pathology*, 262(3):310–319, 2024. doi: 10.1002/path.6232. URL https://doi.org/10.1002/path.6232.

U.S. Bureau of Labor Statistics. Occupational outlook handbook: Data scientists, 2026. URL https://www.bls.gov/ooh/math/data-scientists.htm. Accessed: July 9, 2026. Reported median annual wage: USD $112,590 (May 2024).

B. Vasey, M. Nagendran, B. Campbell, D. A. Clifton, G. S. Collins, S. Denaxas, A. K. Denniston, L. Faes, B. Geerts, M. Ibrahim, X. Liu, B. A. Mateen, P. Mathur, M. D. McCradden, L. Morgan, J. Ordish, C. Rogers, S. Saria, D. S. W. Ting, P. Watkinson, and DECIDE-AI Expert Group. Reporting guideline for the early stage clinical evaluation of decision support systems driven by artificial intelligence: Decide-ai. *BMJ*, 377:e070904, 2022. doi: 10.1136/bmj-2022-070904.

Shayan Vassef, Soorya Ram Shimegekar, Abhay Goyal, Koustuv Saha, Pi Zonooz, and Navin Kumar. One vlm, two roles: Stage-wise routing and specialty-level deployment for clinical workflows, 2025. URL https://arxiv.org/abs/2508.16839.

Shirly Wang, Matthew B. A. McDermott, Geeticka Chauhan, Marzyeh Ghassemi, Michael C. Hughes, and Tristan Naumann. Mimic-extract: a data extraction, preprocessing, and representation pipeline for mimic-iii. In *Proceedings of the ACM Conference on Health, Inference, and Learning*, ACM CHIL '20, page 222–235. ACM, April 2020. doi: 10.1145/3368555.3384469. URL http://dx.doi.org/10.1145/3368555.3384469.

Yanshan Wang, Liwei Wang, Majid Rastegar-Mojarad, Sungrim Moon, Feichen Shen, Naveed Afzal, Sijia Liu, Yuqun Zeng, Saeed Mehrabi, Sunghwan Sohn, and Hongfang Liu. Clinical information extraction applications: A literature review. *Journal of Biomedical Informatics*, 77:34–49, January 2018. doi: 10.1016/j.jbi.2017.11.011. URL https://doi.org/10.1016/j.jbi.2017.11.011.

Yufan Wang, Anit Kumar Sahu, Yan Fei Ng, Daniel Kang, Shayan Vassef, Soorya Ram Shimgekar, Koustuv Saha, Piyum Zonooz, Navin Kumar, Chee Leong Cheng, and Li Yan Khor. Finding H. pylori in the Fine Print: Evidence-Linked Multi-Agent Case Finding from Gastric Biopsy Reports, 2026.

J. H. Wasson, H. C. Sox, R. K. Neff, and L. Goldman. Clinical prediction rules: Applications and methodological standards. *The New England Journal of Medicine*, 313(13):793–799, 1985. doi: 10.1056/NEJM198509263131306.

P. F. Whiting, A. W. Rutjes, M. E. Westwood, S. Mallett, J. J. Deeks, J. B. Reitsma, M. M. Leeflang, J. A. Sterne, P. M. Bossuyt, and QUADAS-2 Group. Quadas-2: A revised tool for the quality assessment of diagnostic accuracy studies. *Annals of Internal Medicine*, 155(8):529–536, 2011. doi: 10.7326/0003-4819-155-8-201110180-00009.

R. F. Wolff, K. G. M. Moons, R. D. Riley, P. F. Whiting, M. Westwood, G. S. Collins, J. B. Reitsma, J. Kleijnen, S. Mallett, and PROBAST Group. Probast: A tool to assess the risk of bias and applicability of prediction model studies. *Annals of Internal Medicine*, 170(1):51–58, 2019. doi: 10.7326/M18-1376.

J. E. Yoo, S. M. Jeong, Y. Yeo, W. Jung, J. Yoo, K. Han, C. M. Lee, J. H. Park, K. W. Park, and D. W. Shin. Smoking cessation reduces the risk of heart failure: A nationwide cohort study. *JACC: Heart Failure*, 11(3):277–287, 2023. doi: 10.1016/j.jchf.2022.07.006.

Appendix A. Supplementary Material

This appendix provides supplementary material referenced throughout the main text but omitted for space. Section A.1 gives the complete point-based scoring rubric underlying all composite features. The remaining subsections provide implementation and evaluation details: EHR source-table schema and preprocessing, model and prompt configurations for the rubric auditor and comorbid-condition discovery, the full LLM construct-validity rubric and results, composite-feature output examples, SHAP feature-importance rankings, the Claude comparator prompt, and the ablation study details and results referenced in Sections 4 and 5.

A.1. Complete Feature Scoring Rubric

Feature	Component	Condition	Points
Disease severity	EF midpoint	< 30 (severely reduced)	35
		30–40 (reduced)	25
		40–50 (mildly reduced)	10
		Missing EF (inferred from DX)	8
	Biomarkers	BNP max ≥ 900	20
		$300 \leq$ BNP max < 900	10
	Troponin	per abnormal result	3 (max 24)
	Procedures	per surgery/procedure	2 (max 12)
		LVAD implantation	18
	Comorbidity	chronic kidney disease (DX)	6
Cardiovascular risk	Age (cont.)	35 (min) to 95 (max)	max 45
	Systolic BP (cont.)	110 (min) to 180 (max)	max 18
	Diastolic BP (cont.)	70 (min) to 110 (max)	max 8
	Risk factor	coronary artery disease (DX)	10
		diabetes (DX)	8
		chronic kidney disease (DX)	8
		hypertension (DX)	6
		hyperlipidemia (DX)	5
		tobacco, current	8
		tobacco, former	3
		alcohol, daily	3
Kidney burden	Primary indicator	chronic kidney disease (DX)	35
		acute kidney failure (DX)	25
	Lab modifier	creatinine abnormalities	4 (max 20)
		latest creatinine > 1.3	5
		latest creatinine > 2.0	10
		electrolyte (Na/K) abnormalities	2 (max 10/type)
	Contextual	diabetes or hypertension (DX)	5 each
Lungs burden	Primary indicator	COPD (DX)	35
		sleep apnea (DX)	25
	Risk context	tobacco, current	12
		tobacco, former	5
		BMI ≥ 35	8
		BMI 30–34.9	4
Metabolic burden	Diagnosis flag	diabetes (DX)	25

continued on next page

Table 3 – continued from previous page

Feature	Component	Condition	Points
		obesity (DX)	20
		hyperlipidemia (DX)	10
		hypertension (DX)	8
	Physical/lab marker	BMI ≥ 35	20
		BMI 30–34.9	12
		glucose abnormalities	3 (max 15)
		latest glucose > 126	5
		latest glucose > 200	10
Blood burden	Primary indicator	anemia (DX)	35
	Lab modifier	hemoglobin abnormalities	5 (max 25)
		hemoglobin < 12	10
		hemoglobin < 10	20
	Contextual	chronic kidney disease modifier	5
Brain-health risk	Scoring factor	age ≥ 75	8
		hypertension (DX)	12
		diabetes (DX)	10
		hyperlipidemia (DX)	8
		sleep apnea (DX)	5
		tobacco, current	8
		alcohol, daily	5
Demographic vulnerability	Language	non-English language	35
	Ethnicity	Hispanic/Latino	15
		unknown/declined	10
	Race	Black or African American	15
		other/unknown/declined	10

Table 3: Complete scoring rubric across all eight point-based aggregated feature categories. Within each category, component points are summed and the total is capped at 100.

```
{
  "disease_severity": {
    "ef_points": [
      {"condition": "ef_midpoint < 30", "points": 35},
      {"condition": "30 <= ef_midpoint <= 40", "points": 25}
    ],
    "severity_cutoffs": {"medium_min": 25, "high_min": 55}
  },
  "cardiovascular_risk": {
    "continuous_components": {
      "age": {"minimum_age": 35, "maximum_age": 95, "maximum_points": 45}
    }
  },
  "medical_grounding": {
    "references": [
      {"journal": "JACC: Heart Failure", "year": 2024,
       "doi": "10.1016/j.jchf.2024.02.020"}
    ]
  }
}
```

Figure 2: Representative slice of the versioned scoring rubric.

A.2. Stage 1 Preprocessing: Source Tables, Deduplication, Aggregation, and Signal Engineering

Table 4 lists the nine EHR-exported source tables described in Section 3, along with example fields from each.

Table 4: EHR-exported source tables

Source table	Description	Example fields
PatientBase	Demographics and core diagnoses	Patient ID, Age, Sex, Race, Ethnicity, Language, BMI, Blood pressure (systolic/diastolic), Pulse, Primary ICD-10 code list, Primary diagnosis name (free text)
OtherDiagnosis	Additional ICD diagnoses	ICD-10 code, diagnosis name, diagnosis date
Medications	Longitudinal medication history	Medication display name, Pharmacologic class, Therapeutic class, Order date
EchoProcs	Echocardiography procedures	Procedure code, Procedure name, Order date
Surgery	Surgical procedures	Procedure name, Procedure date, Hospital, Department
LabsComponents	Internal laboratory data	Laboratory component name, Results date, Units, Abnormal flag, Procedure name
LabsExternal	External laboratory data	Test name, Result value, Units, Abnormal flag, Collection time
EjectionFraction	Ejection fraction recordings	EF value/range (e.g., “25–30%”), Recorded time
SocialHx	Tobacco, alcohol, illicit drug history	Tobacco use, Alcohol use, Illicit drug use

Table 5 lists the deduplication key used for each source table, described in Section 4.

Table 5: Deduplication keys used for EHR source tables.

Source table	Deduplication key
PatientBase	one row per `UNIQUEPATID` (enforced)
OtherDiagnosis	`UNIQUEPATID` + ICD list + DX name
Medications	`UNIQUEPATID` + `ORDERINST` + `MEDICATION_ID`
EchoProcs	`UNIQUEPATID` + `ENCID` + `ORDER_PROC_ID`
Surgery	`UNIQUEPATID` + `ENCID` + `OR_PROC_ID`
Labs (internal + external)	`UNIQUEPATID` + result time + component + value
EjectionFraction	`UNIQUEPATID` + `RECORDED_TIME` + entry
SocialHx	one row per `UNIQUEPATID`

Table 6 lists the patient-level quantities aggregated from each event source before merging, described in Section 4.

Table 6: Patient-level quantities aggregated from each event source before merging.

Source domain	Patient-level aggregates
Medications	Order and distinct-drug counts; first and latest order timestamps; sixteen cardiovascular drug-class flags (e.g., beta blockers, ACE inhibitors, ARBs, ARNI, MRAs, SGLT2 inhibitors, loop diuretics, anticoagulants, inotropes); and derived RAAS and GDMT class counts
Laboratory (internal + external)	Per-analyte counts, abnormal-result counts, maxima, and latest values, with dedicated handling for BNP, NT-proBNP, troponin, electrolytes, creatinine, glucose, and hemoglobin
Surgery	Procedure count and procedure-type indicators (e.g., LVAD, device, valve, catheterization, PCI)
Echocardiography	Procedure count and first/latest order timestamps

Table 7 lists the clinical-reasoning layer that converts raw text and codes into interpretable flags, described in Section 4.

Table 7: Clinical-reasoning layer mapping raw EHR signals to interpretable patient-level features.

Signal	Source	Engineered representation
Cardiovascular comorbidities	ICD-10 codes and diagnosis names	Binary flags from curated pattern sets (e.g., heart failure, coronary artery disease, atrial fibrillation, chronic kidney disease, diabetes, hypertension, COPD)
Behavioral risk	Social history	Ordered categories for tobacco and alcohol use (e.g., current vs. former tobacco use; daily, occasional, past, or no alcohol use)
Biomarkers and advanced therapies	Laboratory results and medications	High-risk biomarker flags (BNP, NT-proBNP, troponin) and advanced-HF therapy flags (e.g., ARNI, SGLT2 inhibitors, inotropes, beta blockers)
Heart-failure phenotype	Diagnosis names and ICD codes	Systolic, diastolic, or combined phenotype with a diagnosis-name/ICD conflict flag

A.3. XGBoost Hyperparameter Configuration

The configuration in Table 8 emphasizes regularization through shallow trees, conservative split criteria, and row and column subsampling to reduce overfitting on the relatively small training set. The same configuration was used for all experiments so that performance differences reflected the feature sets rather than model tuning.

Table 8: Fixed XGBoost hyperparameter configuration used for all downstream classification experiments.

Hyperparameter	**Value**
`max_depth`	3
`n_estimators`	100
`learning_rate`	0.05
`gamma`	1.0
`min_child_weight`	3
`subsample`	0.8
`colsample_bytree`	0.8

A.4. LLM Rubric-Auditor Prompt

The rubric-auditor step (Section 4) uses `Qwen 2.5-1.5B-Instruct` to validate each feature row against patient evidence and correct only whitelisted fields (Table 9). The abbreviated prompt is shown in Figure 3.

Table 9: Whitelisted fields the LLM auditor may correct, versus fields protected from modification.

LLM-correctable	**Protected (never modified)**
Numeric scores, counts, indices, frequencies	Evidence traces (`*_json`)
Indicator / availability flags	Narrative rationales (`*_explanation`)
Fixed set of classification and urgency labels	Patient identifier (`UNIQUEPATID`)

```
You are a rubric auditor. Review the candidate feature row against the patient evidence.

Rules:
1. Use ONLY the patient data.
2. Use ONLY the rubric logic.
3. Do NOT recreate the entire row.
4. If every field is correct return {"valid": true}.
5. If any field is incorrect return
   {"valid": false, "corrections": {"field_name": corrected_value}}.
6. Include ONLY fields that require correction.
7. Never return the entire candidate row.
8. NEVER include any field whose name ends with "_json" or "_explanation".
9. Corrections may only contain scores, counts,
   classifications, urgency labels, indicator flags.
10-11. Do not return explanations or audit JSON.
12. Correction keys must be selected from
    correctable_fields only.

JSON only.

INPUT:
{"patient": {...}, "candidate": {...},
 "correctable_fields": [...]}
```

Figure 3: Abbreviated rubric-auditor prompt

A.5. Comorbid Condition Discovery: Prompt and Example Output

The comorbid condition discovery stage described in Section 4 prompts the language model to select supporting evidence columns for each of the thirteen fixed candidate conditions. Figure 4 shows the abbreviated prompt template for one candidate condition, and Figure 5 shows the representative anemia-candidate output discussed in Section 5.

```
You are creating one row for a condition-level
modeling catalog.

Use only this rubric payload and the listed final
dataset columns.
Do not assign diagnoses to individual patients.
Do not invent condition names, columns, papers,
thresholds, or rules.
Return one JSON object only:

{
  "condition_name": "exact candidate condition name",
  "prediction_columns": ["column_a", "column_b"],
  "explanation": "why these columns support
                  prediction/phenotyping/research
                  flagging"
}

RUBRIC PAYLOAD:
{"rubric_version": "2026-06-16",
 "candidate_condition": {"condition_name":
   "Anemia or hemoglobin abnormality", ...},
 "column_summary": {...}}
```

Figure 4: Abbreviated condition-discovery prompt template for one candidate condition.

```
{
  "condition_name": "Anemia or hemoglobin abnormality",
  "condition_group": "blood",
  "evidence_type": "direct_diagnosis_plus_lab_support",
  "prediction_columns": [
    "dx_anemia", "lab_hemoglobin_count",
    "lab_hemoglobin_abnormal_count", "lab_hemoglobin_latest_value",
    "dx_chronic_kidney_disease", "feature_blood_comorbid",
    "feature_blood_comorbid_score", "feature_kidney_comorbid_score"
  ],
  "explanation": "These columns provide direct and supportive evidence
    for the Anemia or hemoglobin abnormality condition. The 'dx_anemia'
    column indicates whether anemia has been diagnosed, while
    'lab_hemoglobin_count', 'lab_hemoglobin_abnormal_count', and
    'lab_hemoglobin_latest_value' capture hemoglobin levels and their
    variability. [...]"
}
```

Figure 5: Representative comorbid condition-discovery output for the anemia candidate condition.

A.6. LLM Construct-Validity Evaluation

The rubric was developed by clinician and methodology experts based on established prediction-model assessment standards (Collins et al., 2024; Wolff et al., 2019; Kahn et al., 2016; Whiting et al., 2011; Vasey et al., 2022; Wasson et al., 1985; McGinn et al., 2000). These frameworks were synthesized into five independent dimensions: (1) external validation evidence, (2) predictor construction risk, (3) definition and reporting transparency, (4) EHR source data quality, and (5) evidence population and outcome validity. Table 10 reproduces the complete rubric.

Evaluation was performed using Claude Opus 4.8 as an isolated background agent. The model received only the grading rubric and pipeline metadata for each engineered component and was instructed to conduct live web searches for literature supporting each dimension. Unverifiable references were scored as "no verified source found" rather than inferred from model knowledge. Each component received a maximum of 13 points across the five dimensions. Scores were summed within categories and normalized to 0–100 by dividing by the category maximum, 13× the number of components, enabling comparison across categories of different sizes.

Table 10: Five-dimensional rubric used for the LLM-based evaluation of engineered clinical features.

Dimension	**Points**	**Evaluation Criteria**
External Validation Evidence	0–3	Assesses whether the predictor, or a clinically similar proxy, appears in an externally validated multivariable prediction model (e.g., MAGGIC, SHFM, PREVENT, KFRE). Higher scores indicate stronger evidence that the predictor has previously demonstrated prognostic value in validated clinical prediction models.
Predictor Construction Risk	0–3	Evaluates whether the predictor is appropriate for prediction according to PROBAST-inspired principles, including consistent measurement, availability at prediction time, and absence of label leakage. Predictors derived directly or indirectly from outcome-defining variables receive a score of zero.
Definition and Reporting Transparency	0–2	Assesses whether the predictor can be reproduced from the documented implementation, including source variables, computation logic, timing, and handling of missing data.
EHR Source Data Quality	0–3	Evaluates the quality of the underlying structured EHR data using the Kahn data quality framework, assessing conformance to expected formats, completeness of source fields, and clinical plausibility of recorded values.
Evidence Population and Outcome Validity	0–2	Assesses whether supporting literature was conducted in clinically comparable populations using appropriate and reliable outcome definitions or reference standards. Higher scores indicate stronger applicability of the supporting evidence to the intended heart-failure population.
Maximum Total Score	**13**	Sum of all five evaluation dimensions for each engineered component. Category scores are reported as normalized percentages to account for differing numbers of components per category.

To illustrate the evaluation procedure, an excerpt of the LLM system prompt is provided below through Dimension 1 (External Validation Evidence). The excerpt shows the instructions governing feature-level

grading, evidence verification, and the first rubric dimension. The complete evaluation protocol consisted of five dimensions as described in the main text.

SYSTEM

Grade engineered heart-failure pipeline features across five independent dimensions. Every feature belongs to exactly one of 11 categories: `behavioral_risk`, `disease_severity`, `cardiovascular_risk`, `kidney_comorbid`, `lungs_comorbid`, `brain_comorbid`, `metabolic_comorbid`, `blood_comorbid`, `demographic_vulnerability`, `gap`, and `care`.

Each category lists a "components:" line in PIPELINE METADATA naming its individual weighted findings, gap checks, or derived features. The `gap` category consolidates every feature with "gap" or "gap_count" in its name, including `feature_lab_gap_count`, `medication_gap_count`, `surgery_gap_count`, `care_gap_count`, `behavior_aware_care_gap`, `disease_severity_adjusted_gap`, `cv_risk_adjusted_gap`, and `demographic_vulnerability_adjusted_gap`.

These features are grouped together because they are either sums over, or single-formula derivatives of, the same underlying gap checks. The `care` category contains only `feature_care_recommendation_urgency`, which is kept separate from `gap` because it is not itself a gap check or gap-count derivative. No feature is graded standalone outside a category.

Component-level grading.

Grade **EACH** listed component separately (0–13, across the same five dimensions), using the category's shared rubric, citations, implementation notes, and statistics as context. Grade each component's citation, leakage, and transparency independently; do not simply copy one grade across a category.

After grading a category's components, compute the rollup:

$$\texttt{raw_total} = \sum \text{component total_points}$$

$$\texttt{max_possible} = 13 \times \text{number of components}$$

$$\texttt{normalized_score} = \text{round}\left(100 \times \frac{\texttt{raw_total}}{\texttt{max_possible}}, 1\right)$$

The five dimensions are derived from the following methodological frameworks:

1. **External Validation Evidence:** adapted from TRIPOD/PROBAST principles for predictor justification and external validation.
2. **Predictor Construction Risk:** adapted from label leakage and prediction-timing guidance.
3. **Definition and Reporting Transparency:** adapted from TRIPOD reporting recommendations.
4. **EHR Feasibility:** adapted from common EHR feature-engineering and computability principles.
5. **Clinical Plausibility:** adapted from evidence-based clinical prediction-model development and guideline-supported predictors.

For dimensions 1 and 5, every non-zero score must be supported by a verified source (author, year, journal, PMID/DOI if available). If no qualifying source is found, assign 0 (or the lowest applicable band) and state "no verified source found." Never invent citations. For both dimensions, explicitly state whether a literature search was performed.

For pipeline-specific dimensions, use only the provided PIPELINE METADATA. Do not infer undocumented behavior.

Read the entire PIPELINE METADATA before grading. Some metadata blocks document multiple features because they share implementation details; however, each named feature must be graded independently. Shared documentation does not imply identical scores, particularly for Dimension 2, where trigger conditions may differ.

Grade each feature independently without referencing scores assigned to other features. Do not normalize or adjust scores across different features. Process features in metadata order and return exactly 19 output objects in that order.

DIMENSION 1 – External Validation Evidence [0–3]

Evaluate whether this predictor, or a close clinical proxy, appears in an externally validated, multivariable-derived cardiovascular or heart-failure prediction model.

0 = No externally validated multivariable-derived composite score for heart failure or cardiovascular risk includes this predictor or a close clinical proxy.

1 = Appears only in guideline-level evidence, association studies, or single-variable evidence – not in a multivariable-derived score.

2 = Appears as a variable in an externally validated multivariable-derived score (e.g., MAGGIC, SHFM, Framingham, ASCVD/PREVENT, KFRE), but concordance with this pipeline's use cannot be confirmed.

3 = Appears in such a score and the direction and clinical importance of the predictor are broadly concordant with how this pipeline uses and weights the feature. Exact numerical equivalence between published coefficients and pipeline rubric points is not required.

Required output: named score(s), full citation, matched variable name, citation confidence (`verified` | `uncertain` | `not_found`), and whether a literature search was performed. ... *[Prompt excerpt ends here.]*

The model additionally received structured pipeline metadata for each engineered component. An example of the metadata supplied for one feature is shown below.

feature_behavior_risk_score

category: `behavioral_risk`

rubric: `tobacco_current=25` (else `tobacco_former=10`); `alcohol_daily=15` (else `alcohol_current=3`, else `alcohol_past=1`); `illicit_drug_current=25`; `age>=75 +5`; `ef_latest_midpoint_min in (0,40) +8`; and `dx_chronic_kidney_disease`, `dx_diabetes`, and `dx_coronary_artery_disease` each contribute +3.

components: `tobacco_current`, `tobacco_former`, `alcohol_daily`, `alcohol_current_non_daily`, `alcohol_past`, `illicit_drug_current`, `age_75_or_older_modifier`, `ef_below_40_modifier`, `ckd_modifier`, `diabetes_modifier`, `cad_modifier`.

clinical rationale: Estimates lifestyle-related cardiovascular risk, with direct behavioral evidence weighted highest and age, EF, and comorbidity treated as smaller cross-system modifiers.

implementation notes: Tobacco and alcohol variables use hierarchical precedence rules. The temporal EF definition uses the most recent recorded EF rather than the first-recorded or lowest-ever EF.

stats: missing = 0.0%, range = 0–62, mean = 8.3, median = 6.0.

Table 11 reports the resulting category-level construct-validity scores, summarized in Section 5.

Table 11: LLM-based construct-validity evaluation of engineered clinical feature categories. Scores represent summed rubric points across components and normalized category performance relative to the maximum possible score.

Feature Category	**Normalized Score (%)**
Blood Comorbidities	93.8
Cardiovascular Risk	93.4
Brain Comorbidities	91.3
Kidney Comorbidities	90.6
Behavioral Risk	89.5
Lung Comorbidities	88.5
Metabolic Comorbidities	85.5
Disease Severity	74.6
Demographic Vulnerability	63.1
Gap Features	60.6
Care Recommendations	38.5
Overall	**81.5**

A.7. Composite Feature Output Examples

Section 5 describes the two output shapes returned by the higher-order composite features: a scored assessment with ranked drivers, and a list of documentation gaps. Figure 6 shows a representative disease-severity result, and Figure 7 shows a representative care-recommendation result.

```
{
  "severity": "high",
  "severity_score": 55.0,
  "hf_classification": "HFpEF_by_diagnosis_name",
  "hf_classification_source": "DXNAMES",
  "drivers": [
    "HF phenotype inferred from diagnosis text because EF is missing",
    "Markedly elevated BNP/NT-proBNP maximum",
    "Abnormal troponin result burden",
    "CKD comorbidity increases disease complexity"
  ]
}
```

Figure 6: Disease severity feature output.

```
{
  "medications": [
    {"recommendation": "review statin therapy documentation for CAD",
     "evidence_column": "med_statin"}
  ],
  "labs": [
    {"recommendation": "review potassium monitoring availability",
     "evidence_column": "lab_potassium_count"},
    {"recommendation": "review creatinine monitoring availability",
     "evidence_column": "lab_creatinine_count"},
    {"recommendation": "review sodium monitoring availability",
     "evidence_column": "lab_sodium_count"}
  ],
  "surgeries": [],
  "urgency": "high",
  "recommendation_gap_count": 4
}
```


Figure 7: Care recommendation feature output.

A.8. SHAP Feature Importance

Table 12 reports the complete top-10 SHAP feature rankings for both classification tasks, summarized in Section 5.

Table 12: Top 10 features ranked by mean absolute SHAP value for the composite-feature XGBoost models. Larger values indicate greater average contribution to model predictions.

Task	**Feature**	**Mean |SHAP|**
HFrEF	Demographic vulnerability adjusted gap	0.597
	Disease severity adjusted gap	0.456
	HF GDMT medication class count	0.425
	Medication gap count	0.342
	Care gap count	0.322
	Cardiovascular risk adjusted gap	0.307
	Behavior aware care gap	0.229
	Other diagnosis count	0.169
	Medication order count	0.169
	Atrial fibrillation diagnosis	0.141
HFpEF	Disease severity score	0.715
	Troponin abnormal count	0.172
	Troponin max value	0.158
	Other diagnosis count	0.142
	Systolic blood pressure	0.136
	Surgery count	0.117
	Disease severity adjusted gap	0.116
	Weight	0.116
	B-type natriuretic peptide latest value	0.111
	B-type natriuretic peptide max value	0.090

A.9. Claude Comparator Prompt

As an independent comparator, we used Claude Opus 4.8, a state-of-the-art large language model, to determine whether a general-purpose LLM could autonomously engineer clinically meaningful features directly from the same raw EHR data. The model received only the EHR schema, dataset description, and a general instruction to construct features for heart-failure prediction and risk stratification. It was not provided the proposed feature schema, scoring rubric, derived feature categories, or other project-specific implementation details. The comparator was executed once using a single prompt with web search enabled, producing feature-engineering code, documentation, and a patient-level feature matrix without manual modification. The resulting feature set was evaluated using the same baseline variables, XGBoost models, hyperparameters, cross-validation protocol, performance metrics, and construct-validity grading procedure as the proposed framework.

The following prompt was provided to Claude Opus 4.8 to independently generate a patient-level feature dataset from the raw EHR exports.

SYSTEM

You are a data scientist independently building a patient-level feature dataset from fragmented electronic health record (EHR) exports for a heart-failure cohort at an academic medical center.

DATA

You have nine raw relational tables, all keyed on `UNIQUEPATID`. One patient can have multiple rows in most tables, whereas `PatientBase` and `SocialHx` contain one row per patient. Files are located at `[PATH]/baseline_data/`.

- **PatientBase**: `UNIQUEPATID, AGE, PATIENT_SEX, GENDER_IDENTITY, ..., BMI, BP_SYSTOLIC, BP_DIASTOLIC, PULSE, ICD10CODES, DXNAMES`.
- **otherDiagnosis**: `UNIQUEPATID, CURRENT_ICD10_LIST, DX_NAME`.
- **Medications**: `UNIQUEPATID, ORDERINST, MEDICATION_ID, DISPLAY_NAME, PHARMCLASS, THERACLASS`.
- **EchoProcs**: `UNIQUEPATID, ENCID, ORDER_PROC_ID, ORDER_INST, PROC_CODE, PROC_NAME`.
- **surgery**: `UNIQUEPATID, ENCID, SURGERY_DATE, STATUS_C, OR_PROC_ID, PROC_DISPLAY_NAME, ....`
- **LabsComponents**: `UNIQUEPATID, ENCID, ORDER_PROC_ID, ORDER_INST, PROC_CODE, ORDER_PROCNAME, RESULT_TIME, COMPONENT_NAME, ABNORMAL_YN, ORD_VALUE, REFERENCE_UNIT`.
- **LabsExternal**: Same structure as `LabsComponents`, plus `COMPONENT_ID` and `COMMON_NAME`.
- **EjectionFraction**: `UNIQUEPATID, ENCID, DISP_NAME, RECORDED_TIME, FLOWSHEET_ENTRY, ENTRY_COMMENTS`. `FLOWSHEET_ENTRY` contains the raw ejection fraction value or range (e.g., "55", "45–50", "preserved").
- **SocialHx**: `UNIQUEPATID, TOBACCOUSE, ALCOHOLUSE, ILLICITDRUGUSE`.

The original prompt contained the complete column schema for all nine tables. Repetitive column lists have been abbreviated using ... for readability; all instructional content below is reproduced verbatim.

This is a real, de-identified, single-institution EHR export rather than a curated benchmark. Expect duplicate records, inconsistent terminology, free text, and missing observations. Absence of a record means that information was not recorded; it does not necessarily indicate a negative finding. Treat missing and explicitly negative findings as distinct where possible.

PURPOSE

The resulting dataset will be used for downstream heart-failure prediction and risk-stratification tasks. Prioritize features that plausibly capture clinically meaningful information relevant to predicting heart-failure risk.

TASK

Build a single patient-level dataset with exactly one row per `UNIQUEPATID`.

First, consolidate the nine tables by independently determining deduplication and aggregation strategies for diagnoses, medications, laboratory results, procedures, ejection-fraction measurements, and other repeated records.

Second, independently engineer additional patient-level features that you consider clinically useful for predicting and risk-stratifying heart failure. You may transform, combine, aggregate, or summarize any available variables. Determine the feature definitions, representations, thresholds, and aggregation strategies yourself.

You are intentionally *not* given a predefined feature schema, feature categories, scoring rubric, prediction target, or target feature count. Do not attempt to reproduce any existing feature-engineering framework.

Composite features should be included when they provide a clinically meaningful representation that is not adequately captured by their individual components rather than being included purely for descriptive completeness.

Where useful, you may use web search to verify clinical definitions or thresholds. Restrict searches to general peer-reviewed clinical and biomedical literature.

REQUIREMENTS

- Implement the complete workflow as runnable Python using `pandas`.
- Every feature must be generated deterministically from the provided EHR data.
- Do not invent, hallucinate, or assign patient information not supported by the source data.
- Do not use `UNIQUEPATID`, row order, or database artifacts as features.
- Missing information must not automatically be interpreted as a negative clinical finding.
- Prioritize clinically meaningful and interpretable features rather than maximizing feature count.
- Document all deduplication, aggregation, and feature-engineering decisions.

For every derived feature, document:

- what it measures;
- source table(s) and column(s);
- how it is computed;
- how missing data are handled;
- any clinical assumptions or thresholds used;
- supporting literature citation, if verified through an allowed literature search.

OUTPUTS

Produce:

1. `comparator_features.csv` containing one row per `UNIQUEPATID` with the consolidated patient-level variables and independently engineered features.
2. `comparator_feature_documentation.md` documenting all aggregation and derived-feature decisions.
3. The Python script used to generate both outputs.

Before finishing, verify that the CSV contains exactly one row per `UNIQUEPATID`.

Inspection of the comparator features showed that the LLM followed a different feature-engineering strategy from the proposed framework. Given only the raw EHR tables, it primarily generated features based on directly observed clinical variables, including ICD-10 diagnosis patterns, ejection-fraction measurements, medication use, laboratory values, and procedure history. Examples included ICD-10-derived heart-failure phenotype and acuity indicators, a guideline-directed medical therapy (GDMT) medication count, an ICD-10 adaptation of the Charlson Comorbidity Index, laboratory abnormality indicators, and healthcare utilization

measures such as echocardiography frequency. Several of these features were clinically meaningful. However, features derived from heart-failure diagnosis codes and ejection-fraction measurements received lower construct-validity scores because they were closely related to the classification labels themselves, creating predictor-construction concerns. Additionally, utilization-based features captured patterns of care delivery rather than independently validated markers of disease severity. These findings demonstrate that generating clinically plausible features alone does not guarantee features that are independent, evidence-grounded, and suitable for downstream prediction.

A.10. Ablation Details

Eight targeted modifications were applied independently to the full feature-engineering pipeline to assess the contribution of individual feature categories and design choices. For each ablation, synthetic features were regenerated using the modified scoring logic and evaluated using the identical XGBoost training and cross-validation pipeline as the full aggregated model. This design isolates the contribution of each feature component or scoring decision by ensuring that observed performance differences arise only from the targeted ablation.

Table 13: Ablation configurations evaluated in the sensitivity analysis.

Configuration	Description
Category ablation	Excludes all features within a composite feature category to assess its contribution.
Feature ablation	Excludes one feature at a time to assess individual feature contributions.
Equal-weight rubric	Replaces clinician-derived point values with equal feature weights.
Random-weight rubric	Replaces clinician-derived point values with randomized weights.
No modifiers	Removes cross-system comorbidity modifiers (CKD, diabetes, CAD, and hypertension) from their respective category scores.
Uniform modifiers	Assigns a fixed 1-point weight to all cross-system modifiers to assess the contribution of modifier presence independent of magnitude.
No missingness guardrails	Removes availability indicators and imputes missing continuous variables to assess the effect of distinguishing unmeasured from measured-normal values.
Direct evidence only	Restricts features to diagnoses and direct measurements, excluding supportive laboratory findings, behavioral factors, and cross-system modifiers.

Because repeated-CV folds reuse the same patients under different partitions and are therefore not independent trials, significance is assessed with the corrected resampled paired t-test of Nadeau and Bengio (2003), which inflates the variance estimate by $(1/k + n_{\text{test}}/n_{\text{train}})$ to avoid overstating confidence from correlated fold-level measurements.

A.11. Ablation Results

Category-level ablation identified the clinical domains contributing most to classification performance (Table 15). For HFrEF, removing care-gap features produced the largest performance reduction (ΔAUROC=-0.039), whereas other category removals had minimal effects. For HFpEF, disease severity was the dominant contributor (ΔAUROC=-0.033), consistent with the importance of phenotype-specific evidence. Individual feature ablations, reported below, showed similar patterns with smaller effects, suggesting that performance gains arose from combining related clinical evidence rather than dependence on single features.

Table 14: Rubric design ablation results relative to the full aggregated model.

Ablation	**Modification**	**HFrEF**		**HFpEF**	
		ΔAUROC	p	ΔAUROC	p
Equal-weight rubric	Replaces clinician-assigned weights with equal component weighting.	-0.060	0.0059	-0.041	0.0007
Random-weight rubric	Replaces clinician-assigned weights with randomized weights.	-0.058	0.0070	-0.040	0.0010
No modifiers	Removes cross-system comorbidity modifiers.	-0.001	0.748	-0.000	0.779
Uniform modifiers	Sets all modifiers to a fixed 1-point contribution.	-0.000	0.936	-0.001	0.928
No missingness guardrails	Removes availability indicators and imputes missing values.	+0.001	0.749	+0.007	0.607
Direct evidence only	Removes supportive evidence and retains direct measurements only.	-0.065	0.0037	-0.040	0.0003

Table 15: Category-level ablation results relative to the full aggregated model. ΔAUROC represents the change in mean test AUROC relative to the full model. Negative values indicate reduced performance after category removal.

Removed feature category	**HFrEF ΔAUROC**	**HFpEF ΔAUROC**
Care gap features	-0.039	-0.003
Disease severity	-0.000	-0.033
Brain comorbid burden	+0.001	-0.002
Recurrence/redundancy	-0.001	-0.001
Metabolic comorbid burden	-0.001	-0.001
Demographic vulnerability	-0.001	-0.000
Kidney comorbid burden	-0.000	-0.000
Lung comorbid burden	-0.001	+0.001
Blood comorbid burden	+0.001	+0.001
Cardiovascular risk	+0.000	+0.001
Behavioral risk	-0.001	+0.003

A.12. Individual Feature Ablation

Table 16: Individual feature ablation results for HFrEF classification.

Feature category	**Removed feature**	**ΔAUROC**
Metabolic comorbid burden	feature_metabolic_comorbid_score	-0.002
Behavioral risk	feature_behavior_risk_score	-0.001
Demographic vulnerability	feature_demographic_vulnerability_score	-0.001
Lung comorbid burden	feature_lungs_comorbid_score	-0.000
Care gap	feature_lab_gap_count	-0.000
Care gap	feature_surgery_gap_count	-0.000
Brain comorbid burden	feature_brain_comorbid_score	-0.000
Care gap	feature_care_gap_count	-0.000
Disease severity	feature_disease_severity_score	-0.000
Blood comorbid burden	feature_blood_comorbid_score	-0.000
Care gap	feature_medication_gap_count	+0.000
Care gap	feature_behavior_aware_care_gap	+0.000
Cardiovascular risk	feature_cardiovascular_risk_score	+0.000
Kidney comorbid burden	feature_kidney_comorbid_score	+0.000
Care gap	feature_demographic_vulnerability_adjusted_gap	+0.001

Table 17: Individual feature ablation results for HFpEF classification.

Feature category	**Removed feature**	**ΔAUROC**
Disease severity	feature_disease_severity_score	-0.033
Care gap	feature_disease_severity_adjusted_gap	-0.003
Care gap	feature_surgery_gap_count	-0.002
Care gap	feature_lab_gap_count	-0.001
Kidney comorbid burden	feature_kidney_comorbid_high	-0.001
Care gap	feature_medication_gap_count	-0.001
Kidney comorbid burden	feature_kidney_comorbid_score	-0.001
Care gap	feature_behavior_aware_care_gap	-0.001
Care gap	feature_demographic_vulnerability_adjusted_gap	-0.001
Care gap	feature_care_gap_count	-0.001
Metabolic comorbid burden	feature_metabolic_comorbid_nan	-0.001
Kidney comorbid burden	feature_kidney_comorbid_medium	-0.001
Kidney comorbid burden	feature_kidney_comorbid_nan	-0.000
Lung comorbid burden	feature_lungs_comorbid_low	-0.000
Lung comorbid burden	feature_lungs_comorbid_nan	-0.000